horticulturae

MDPI

Article

Optimized Spectral and Spatial Design of High-Uniformity and Energy-Efficient LED Lighting for Italian Lettuce Cultivation in Miniature Plant Factories

Zihan Wang, Haitong Huang, Mingming Shi *, Yuheng Xiong, Jiang Wang, Yilin Wang and Jun Zou *

College of Science, Shanghai Institute of Technology, No. 100, Haiquan Road, Fengxian District, Shanghai 201418, China; 236182115@mail.sit.edu.cn (Z.W.); 246182127@mail.sit.edu.cn (Y.X.)
* Correspondence: mmshi@sit.edu.cn (M.S.); zoujun@sit.edu.cn (J.Z.)

Abstract

Optimizing artificial lighting in controlled-environment agriculture is crucial for enhancing crop productivity and resource efficiency. This study presents a spectral–spatial co-optimization strategy for LED lighting tailored to the physiological needs of Italian lettuce (*Lactuca sativa* L. var. italica). A miniature plant factory system was developed with dimensions of 400 mm × 400 mm × 500 mm (L × W × H). Seven customized spectral treatments were created using 2835-packaged LEDs, incorporating various combinations of blue and violet LED chips with precisely controlled concentrations of red phosphor. The spectral configurations were aligned with the measured absorption peaks of Italian lettuce (450–470 nm and 640–670 nm), achieving a spectral mixing uniformity exceeding 99%, while the spatial light intensity uniformity surpassed 90%. To address spatial light heterogeneity, a particle swarm optimization (PSO) algorithm was employed to determine the optimal LED arrangement, which increased the photosynthetic photon flux density (PPFD) uniformity from 83% to 93%. The system operates with a fixture-level power consumption of only 75 W. Experimental evaluations across seven treatment groups demonstrated that the E-spectrum group—comprising two violet chips, one blue chip, and 0.21 g of red phosphor—achieved the highest agronomic performance. Compared to the A-spectrum group (three blue chips and 0.19 g of red phosphor), the E-spectrum group resulted in a 25% increase in fresh weight (90.0 g vs. 72.0 g), a 30% reduction in SPAD value (indicative of improved light-use efficiency), and compared with Group A, Group E exhibited significant improvements in plant morphological parameters, including a 7.05% increase in plant height (15.63 cm vs. 14.60 cm), a 25.64% increase in leaf width (6.37 cm vs. 5.07 cm), and a 6.35% increase in leaf length (10.22 cm vs. 9.61 cm). Furthermore, energy consumption was reduced from 9.2 kWh (Group A) to 7.3 kWh (Group E). These results demonstrate that integrating spectral customization with algorithmically optimized spatial distribution is an effective and scalable approach for enhancing both crop yield and energy efficiency in vertical farming systems.

Keywords: LED spectral customization; miniature plant factory; PSO optimization; PPFD uniformity; energy efficiency; absorption-guided lighting design

check for updates

Academic Editor: Angelo Signore

Received: 29 May 2025
Revised: 17 June 2025
Accepted: 25 June 2025
Published: 3 July 2025

Citation: Wang, Z.; Huang, H.; Shi, M.; Xiong, Y.; Wang, J.; Wang, Y.; Zou, J. Optimized Spectral and Spatial Design of High-Uniformity and Energy-Efficient LED Lighting for Italian Lettuce Cultivation in Miniature Plant Factories. *Horticulturae* **2025**, *11*, 779. https://doi.org/10.3390/horticulturae11070779

Copyright: © 2025 by the authors. Licensee MDPI, Basel, Switzerland. This article is an open access article distributed under the terms and conditions of the Creative Commons Attribution (CC BY) license (https://creativecommons.org/licenses/by/4.0/).

1. Introduction

Lactuca sativa var. italica, commonly known as Italian lettuce, is a leafy vegetable widely cultivated in controlled-environment agriculture (CEA) systems due to its rapid

growth cycle, compact morphology, and high market demand. Its responsiveness to light quality and quantity makes it an ideal model species for evaluating the performance of artificial lighting systems in plant factories. As highlighted by He et al. (2020), lettuce varieties, particularly *Lactuca sativa*, serve as standard crops for optimizing light strategies, nutrient delivery, and spatial configuration in vertical farming environments due to their sensitivity to environmental fluctuations and measurable physiological traits [1]. Therefore, studying Italian lettuce under varied spectral–spatial light distributions can provide valuable insights for enhancing productivity and energy efficiency in indoor cultivation systems.

The spectral absorption characteristics of lettuce are critical for understanding its light requirements and optimizing growth conditions, particularly in controlled-environment agriculture (CEA). The current methods involve physical testing to determine these characteristics, but large-scale experiments aimed at selecting appropriate spectra for lettuce can be prohibitively costly and energy-consuming, thereby restricting research efficiency and practical application in agriculture [1]. One of the significant challenges facing contemporary CEA is the uneven distribution of supplementary lighting, which negatively impacts light penetration and ultimately the consistency of plant growth. This issue can lead to variability in crop quality and yield, making it essential to develop solutions that enhance lighting uniformity across the plant canopy [2]. Various studies highlight the importance of light intensity, spectrum, and distribution in determining the growth dynamics of lettuce, emphasizing that discrepancies in these parameters can lead to uneven growth and nutrient concentration throughout the plants [3]. To address this, studies have investigated phosphor-converted LEDs and spectrum evaluation metrics such as SRPAS (Spectrum Resemblance to Plant Absorption Spectrum), which quantifies how closely a light source matches plant-specific absorption characteristics [4]. Although this offers a path toward more tailored light spectra, conducting large-scale, multi-spectral cultivation experiments remains costly and energy-intensive—especially when seeking to optimize for specific crops, growth stages, or canopy structures. In parallel, another critical yet often overlooked factor in plant factory lighting is spatial light uniformity. Standard LED arrays based on uniform grids frequently produce non-uniform PPFD (photosynthetic photon flux density) distributions, leading to growth inconsistencies across the canopy and inefficient use of photons [5,6]. This becomes even more critical in miniature plant factories, where space constraints amplify the impact of uneven illumination. Light-use efficiency (LUE), defined as the ratio of biomass accumulation to the quantity of absorbed photosynthetically active radiation (PAR), is a key metric for evaluating the performance of lighting strategies in controlled-environment agriculture (CEA). It offers a quantitative basis for assessing the trade-off between energy consumption and crop productivity. Briglia et al. (2024) emphasized that optimizing LUE is essential for reducing operational costs while maintaining high crop yields, especially in energy-intensive vertical farming systems [7]. Similarly, Baeza et al. (2022) highlighted that variations in light spectrum and spatial distribution significantly affect LUE by altering photosynthetic efficiency and plant morphology [8]. Incorporating LUE into lighting system design not only supports sustainable production goals, but also enhances decision-making in spectral optimization, fixture layout, and energy management in plant factories.

To overcome both spectral mismatch and spatial non-uniformity, algorithm-driven lighting design presents a compelling solution. In particular, particle swarm optimization (PSO) has been applied to optimize LED arrangements for improving light uniformity and reducing wasted energy [9]. By integrating plant-specific absorption spectra into the optimization process, it is possible to design lighting systems that simultaneously match spectral needs, improve PPFD uniformity, and enhance energy efficiency.

Several studies have explored the application of LED lighting systems for lettuce cultivation, often focusing on either spectral composition or energy consumption. Therefore, by integrating spectral suitability with spatial optimization, our system achieves both physiological effectiveness and energy conservation. This dual-targeted approach addresses current limitations in LED plant lighting design, especially in space-constrained miniature plant factories [10,11].

This study aims to develop a PSO-optimized LED lighting system for the efficient cultivation of Italian lettuce in miniature plant factories. We integrate spectral design principles based on lettuce's known absorption spectrum with spatial layout optimization to enhance both light-use efficiency and growth uniformity. The system is validated through a combination of optical simulations and physiological measurements under nine distinct spectral treatments, providing a data-driven pathway toward more sustainable and precise plant lighting strategies.

2. Materials and Methods

2.1. Plant Lighting Metrics and Uniformity

Plant lighting predominantly relies on a measurement system for photosynthetically active radiation (PAR), which is crucial for photosynthesis as it corresponds to the energy from solar radiation that plants can utilize. In addition to PAR, the photosynthetic photon flux (PPF), measured in μmol/s, indicates the total number of photons in the PAR range that are available to plants per second. PAR measurement systems can be categorized into three main types: optical systems, energy systems, and quantum systems. These systems are represented by light illumination (lm/m^2), radiation illumination (W/m^2), and optical quantum density (μmol/m^2/s), respectively. Notably, while PAR flux density (W/m^2) quantifies energy per unit area, PPFD (μmol/m^2/s) reflects photon count per unit area and time. Because photon energy is inversely proportional to wavelength, the conversion between these units depends on the spectral distribution of the light source. In this study, PPFD was used as the primary metric to evaluate plant lighting performance, as it directly corresponds to the photon quantity available for photosynthesis. Below, the relationships among these metrics, including PPF, are discussed [12–14].

- Conversion Relationship between Radiant E_e and Luminous Illuminance E_v

  The PAR illuminance E_e represents the radiation energy per unit time:

$$E_e = \int E_e(\lambda)\mathrm{d}\lambda. \tag{1}$$

In a quantum system, radiation energy can be interpreted as the product of the number of photons and the energy associated with each photon. When the photosynthetic photon flux density (PPFD), measured in μmol/m^2·s, is denoted as U, the number of photons per mole is represented by n_p. Therefore, irradiance can be expressed as follows:

$$n_p = \frac{1}{h_p c}\int \lambda E_e(\lambda)\mathrm{d}\lambda, \tag{2}$$

$$n_p = U \cdot N_A \cdot 10^{-6}, \tag{3}$$

In this context, $h = 6.626 \times 10^{-34}$ h represents Planck's constant, $c = 3 \times 10^8$ indicates the speed of light, and $N_A = 6.022 \times 10^{23}$ is Avogadro's constant. The relationship between radiant illuminance E_e and photon flux density U can be derived as follows:

$$E_e = N_A \cdot hc \cdot U\frac{\int E_e(\lambda)\mathrm{d}\lambda}{\int \lambda E_e(\lambda)\mathrm{d}\lambda}. \tag{4}$$

The relationship between radiant E_e and luminous illuminance E_v can be transformed by the visual function $V(\lambda)$:

$$E_v = \frac{K_m \int V(\lambda) E_e(\lambda) \mathrm{d}\lambda}{\int E_e(\lambda) \mathrm{d}\lambda} \cdot E_e, \tag{5}$$

where K_m is a constant and $V(\lambda)$ represents the visual function of the human eye. By combining Equations (4) and (5), the conversion relationship between illuminance E_v and photon flux density U can be derived as follows:

$$E_v = U \cdot \frac{N_A \cdot b \cdot c \cdot K_m \int V(\lambda) E_e(\lambda) \mathrm{d}\lambda}{\int \lambda E_e(\lambda) \mathrm{d}\lambda}. \tag{6}$$

- Illumination Uniformity

In the field of plant photometry, plant responses to light primarily involve photosynthetic PPFD and spectral components. Among these, PPFD uniformity and spectral uniformity are also referred to as illuminance uniformity and color-mixing uniformity. Based on Equation (6), it can be inferred that the optical quantum flux density U and its uniformity on the target plane can be expressed as follows [15]:

$$\begin{aligned} \delta &= \frac{\sum_{x=1}^{X} \sum_{y=1}^{Y} \sum_{n=1}^{N} U/(X \cdot Y \cdot Z)}{K_{\mathrm{PPFDmax}}} \\ &= \frac{\frac{1}{K_m} \sum_{x=1}^{X} \sum_{y=1}^{Y} \sum_{n=1}^{N} E_v/(X \cdot Y \cdot Z)'}{\frac{1}{K_m} E_{\mathrm{vmax}}}. \end{aligned} \tag{7}$$

In Equation (7), K_m is a constant, and X and Y refer to the length and width of the receiving surface, respectively. The variable N indicates the number of measurement points on the plane. This suggests that the PPFD uniformity, which can be difficult to assess, can be effectively represented by illuminance uniformity.

- PPF Utilization Efficiency (PPFUE)

Photosynthetic photon flux utilization efficiency (PPFUE) is an important metric that measures the efficiency with which plants utilize the photosynthetic photon flux (PPF) received from a light source. Specifically, it represents the ratio of the average PPF on the plant surface to the total PPF emitted by the light source [16].

$$\mathrm{PPF}_{avg} = \frac{1}{A} \int_A PPFD dA \tag{8}$$

where PPFD is measured in μmol/m^2·s.

The total PPF emitted by the light source (PPF source) is defined as the total number of photons emitted per second by the light fixture. This can typically be provided by the manufacturer or measured directly:

$$\mathrm{PPF}_{source} = U \cdot A \tag{9}$$

where U is the PPF emitted per unit area (μmol/m^2·s) and A is the area over which the light is emitted.

$$\mathrm{PPFUE} = \frac{\int_A PPFD dA}{U \cdot A^2} \tag{10}$$

2.2. System Design and LED Optimization

To replicate the operational characteristics of full-scale plant factories in a compact and energy-efficient form, we developed a miniature plant factory system with dimensions

of 400 mm × 400 mm × 500 mm (L × W × H). This system serves as a scaled-down version of a modern commercial plant factory, incorporating essential environmental control functionalities such as adjustable temperature, humidity, irrigation, and nutrient supply. The enclosed structure is designed to ensure environmental stability and isolation from ambient fluctuations, enabling repeatable and precise evaluation of lighting strategies on crop performance. To further enhance experimental accuracy, the growth chamber is equipped with external light shielding, and the inner walls are coated with non-reflective, light-absorbing material. This design eliminates stray reflections and prevents external light interference, ensuring that all photon exposure originates solely from the tested LED system. The supplemental lighting unit—optimized using PSO—is mounted 50 cm above the plant canopy within this enclosed structure, simulating realistic cultivation conditions under fully controllable environmental and photonic settings. The schematic diagram of the supplementary lighting system in the miniature plant factory is shown in Figure 1a, while Figure 1b illustrates the light supplement setup after shading treatment.

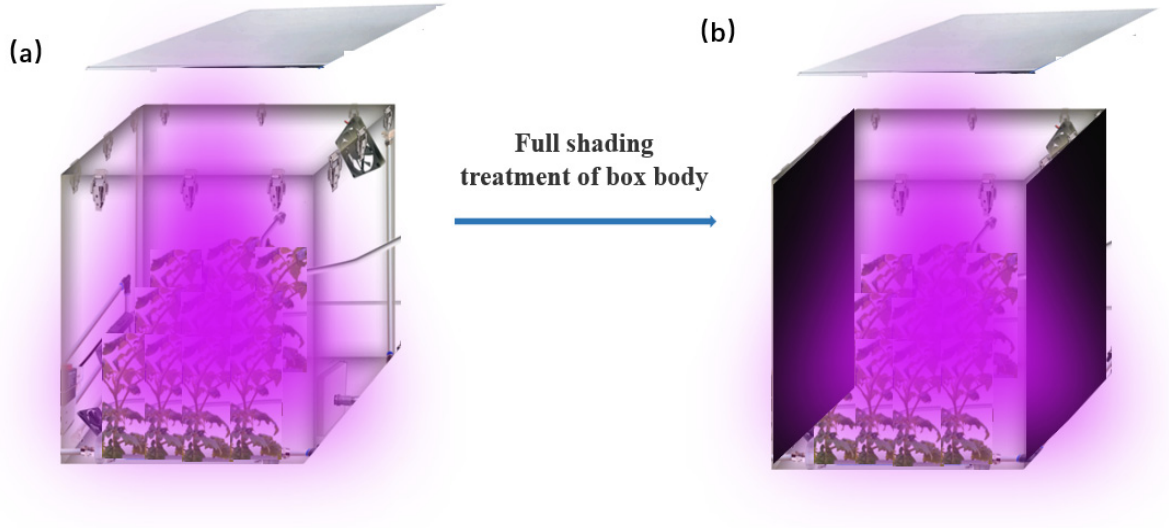


Figure 1. (**a**) Schematic diagram of supplementary light in a miniature plant factory; (**b**) schematic diagram of light supplement after shading treatment for a miniature plant factory.

Following the optimization phase, the refined design was validated through optical simulations in TracePro (Lambda Research Corporation, Littleton, MA, USA), adhering to the fundamental standards and measurement protocols established by the International Commission on Illumination (CIE). In the simulation model, the horticultural lighting fixture was designed with dimensions of 360 mm × 360 mm × 1 mm, featuring a receiving surface of 400 mm × 400 mm positioned 500 mm from the fixture's light-emitting surface. The LED lighting module comprises 360 custom-fabricated LED chips using 2835 surface-mount packaging. All LEDs were manufactured with a uniformly customized emission spectrum, specifically tailored to match the absorption characteristics of lettuce. The chips are non-uniformly distributed across the fixture, with increased density at the periphery to minimize edge-effect photon loss and improve uniformity. To ensure optimal spectral integration, the system was designed and verified to achieve a spectral mixing uniformity of 99% across the target cultivation area. In the optical simulation, each LED chip was modeled to emit 10,000 rays, allowing for high-resolution analysis of spatial PPFD distribution and photon flux overlap.

The PSO algorithm is a population-based optimization method that iteratively refines potential solutions based on individual and global best evaluations [17]. Rather than independently optimizing the position of each LED bead, which could lead to irregular

array configurations and increased manufacturing complexity, this study concentrates on optimizing the row and column spacing of the LED array as the primary variables. Each particle in the PSO algorithm represents a potential LED arrangement, characterized by row spacing (x_{k1}, x_{k2}, . . ., $x_{k(i-1)}$) and column spacing (x_{k1}, x_{k2}, . . ., $x_{k(j-1)}$). The PSO algorithm was implemented in Python 3.7 to iteratively determine the optimal LED spacing for maximizing PPFD uniformity. The initial population consisted of 50 particles, each representing a candidate LED arrangement. To maintain practical constraints, the maximum array dimensions were set at Lmax = 360 mm and Wmax = 360 mm, with a minimum allowable row–column spacing (r = 5 mm) to ensure adequate LED separation and heat dissipation. Figure 2 illustrates the logic design of the particle swarm optimization algorithm.

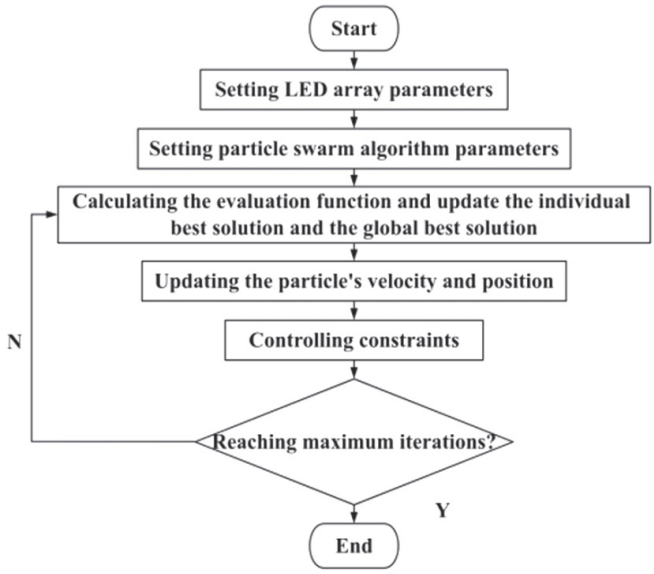


Figure 2. This flowchart outlines the particle swarm optimization (PSO) process for improving light distribution uniformity. The decision point determines whether the current iteration count has reached the specified maximum; "N" (No) prompts continued iteration, while "Y" (Yes) indicates convergence or termination of the algorithm.

The best solution for each particle (Pbest) and the global best solution (Gbest) were determined based on the lowest evaluation function values. The position and velocity of each particle were iteratively updated using the following equations:

Each particle in the PSO algorithm represents a potential LED arrangement, characterized by row spacing (x_{k1}, x_{k2}, . . ., $x_{k(i-1)}$) and column spacing (x_{k1}, x_{k2}, . . ., $x_{k(j-1)}$). The velocity update is governed by:

$$V_k^{n+1} = w \cdot V_k^n + c_1 \cdot rand(0,1) \cdot (Pbest - X_k^n) + c_2 \cdot rand(0,1) \cdot (Gbest - X_k^n) X_k^{n+1} = X_k^n + V_k^{n+1} \quad (11)$$

where w = 0.5 is the inertia weight, controlling velocity inheritance; $c_1 = c_2 = 1.49$ are acceleration coefficients, balancing exploration and convergence; and rand (0, 1) introduces stochasticity to avoid premature convergence. Figure 3a shows the LED lamp board designed using the particle swarm optimization algorithm under a 360 mm × 360 mm substrate, while Figure 3b presents the traditional LED arrangement on the same substrate.

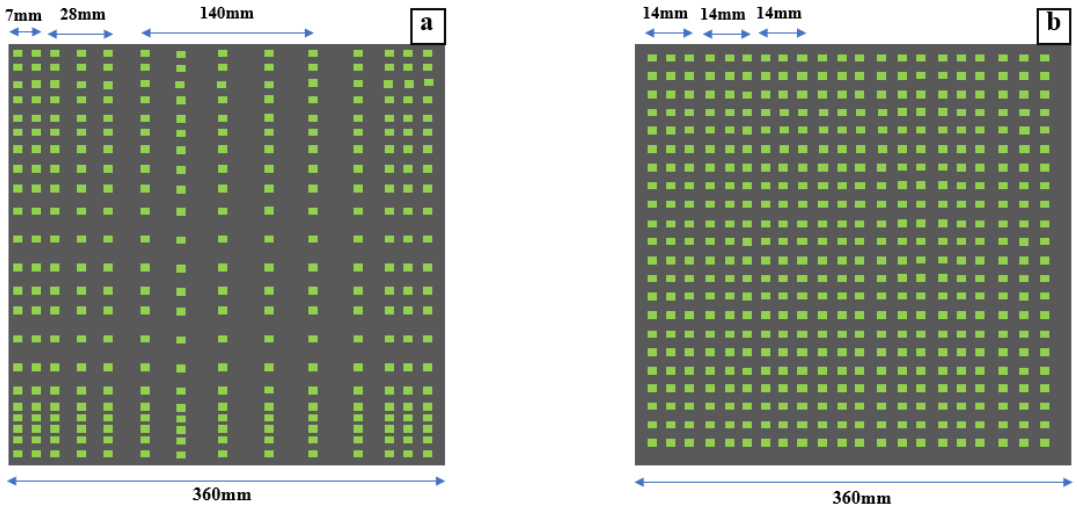


Figure 3. (**a**) LED lamp board designed by the particle swarm algorithm under 360 mm × 360 mm substrate; (**b**) lamp board designed with a traditional LED arrangement under a 360 mm × 360 mm substrate.

The signal-to-noise ratio (SNR) is employed to quantify quality characteristics derived from simulation results, facilitating the identification of optimal solutions. In this experiment, the "larger-the-better" characteristic of the SNR serves as the criterion for evaluating illumination uniformity; specifically, a higher SNR value indicates greater uniformity. The formula for calculating the SNR is provided in the referenced literature [18–20].

$$L_{\mathrm{TB}}\frac{S}{N} = -10log\frac{\sum_{i=1}^{n}\frac{1}{y_i^2}}{n} \tag{12}$$

2.3. Spectral Design for Italian Lettuce

Seven custom spectral profiles were designed and fabricated for this study, all based on uniformly customized LED chips. Table 1 shows the distribution of seven different light qualities.

Table 1. Distribution of light quality of different groups.

Group	Light Configuration
A	3 blue chips + 0.19 g red phosphor
B	3 blue chips + 0.21 g red phosphor
C	3 blue chips + 0.23 g red phosphor
D	3 blue chips + 0.25 g red phosphor
E	2 violet chips + 1 blue chip + 0.21 g red phosphor
F	1 violet chip + 2 blue chips + 0.21 g red phosphor
G	Full-spectrum LED

All LED chips utilized in the lighting system were of the 2835 package type, featuring a 120° beam angle. Each chip operated at a rated voltage of 8.9 V and a current of 100 mA. The same electrical and optical configuration was applied across all treatments to ensure consistency, with spectral differences achieved through chip and phosphor variation. Each spectral group was produced using 2835-packaged LEDs with verified emission peaks. The spectral power distributions of each lighting type were confirmed using a spectroradiometer (PLA-30), ensuring consistency with the design targets. The seven customized spectral treatments used in this study are illustrated in Figure 4, including red:blue ratios ranging

from 6:4 to 9:1 and mixed red: blue: purple compositions, as well as a full-spectrum white LED array as the baseline.

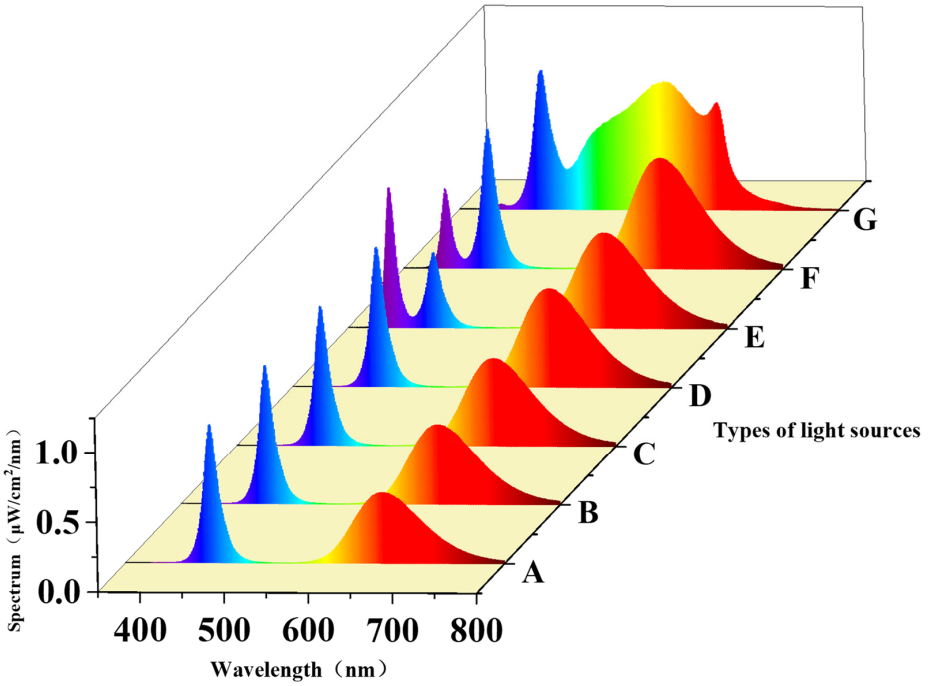


Figure 4. Seven customized spectra. Group A: red:blue (R:B) = 6:4 (3 blue chips + 0.19 g red phosphor); Group B: red:blue (R:B) = 7:3 (3 blue chips + 0.21 g red phosphor); Group C: red:blue (R:B) = 8:2 (3 blue chips + 0.23 g red phosphor); Group D: red:blue (R:B) = 9:1 (3 blue chips + 0.25 g red phosphor); Group E: red:blue:purple (R:B:P = 6:2:2) (2 violet chips + 1 blue chip + 0.21 g red phosphor); Group F: red:blue:purple (R:B:P) = 6:3:1 (1 violet chip + 2 blue chips + 0.21 g red phosphor); Group G: full-spectrum white LED array (baseline reference).

Prior to biological experimentation, an optical simulation was conducted to compare the spatial light distribution of a PSO-optimized LED panel (System A) with that of a conventional uniform LED array (System B). All subsequent plant growth experiments were conducted exclusively under the PSO-optimized lighting system. Seven customized spectral treatments were applied, each designed based on the measured absorption characteristics of Italian lettuce. These treatments included varying combinations of blue and violet LED chips with specific red phosphor concentrations, as well as a full-spectrum white LED control. All treatments were conducted under standardized environmental conditions, with a 12 h light/12 h dark photoperiod and a constant canopy-level PPFD of 200 μmol·m^{-2}·s^{-1}. This design enabled the isolated evaluation of the effects of spectral composition effects on lettuce growth and physiological responses under a spatially optimized lighting regime.

2.4. Plant Material and Data Collection Methods

The test crop was Italian lettuce (*Lactuca sativa* var. italica), cultivar 'Green Coral,' obtained from Shanghai Jiafeng Seed Co., Ltd., Shanghai, China. The plants were grown using a deep-flow hydroponic system without any solid substrate. The nutrient solution was based on a modified Hoagland formulation containing 7.5 mM NO_3^-, 1.0 mM NH_4^+, 1.0 mM $H_2PO_4^-$, 4.0 mM K^+, 2.0 mM Ca^{2+}, 0.5 mM Mg^{2+}, and micronutrients including Fe-EDTA (0.1 mM), Mn^{2+}, Zn^{2+}, B^{3+}, and MoO_4^{2-}. The pH was maintained at 5.8 ± 0.2, and electrical conductivity (EC) was controlled at 2.0 mS·cm^{-1} throughout the cultivation period.

Italian lettuce (*Lactuca sativa* L.) was cultivated in a custom-designed miniature plant factory situated within a climate-controlled growth chamber. Each cultivation tray comprised 12 hydroponic planting slots arranged in a 3-row by 4-column configuration. Plants were spaced at 4 cm intervals both horizontally and vertically, facilitating high-density planting while ensuring adequate air circulation and minimizing mutual shading. The total effective planting area per tray was 38 cm by 30 cm. A substrate-free deep-flow hydroponic method was employed, with roots suspended in a circulating nutrient solution. The electrical conductivity (EC) was maintained at 2.0 $mS \cdot cm^{-1}$ to ensure sufficient nutrient availability throughout the growth period. The solution was aerated and replenished regularly to prevent oxygen or nutrient limitations. The environmental conditions during the experiment were controlled as follows:

- Air temperature: 20 ± 2 °C;
- Relative humidity: 60% to 70%.

CO_2 concentration: Maintained at approximately 800 ppm through CO_2 enrichment to promote photosynthetic efficiency. To comprehensively assess the growth and physiological responses of Italian lettuce under different LED spectral treatments, a multi-parameter monitoring strategy was implemented. Each miniature plant factory tray housed 12 plants, and for each measurement, 6 plants were randomly selected to ensure representative sampling. For every selected plant, each parameter was measured three times, and the average value was used for data analysis to improve precision and reliability.

Plant height, leaf width, and leaf length were recorded weekly using standard rulers and digital calipers, providing continuous quantitative indicators of vegetative development. Chlorophyll content, a proxy for photosynthetic capacity and nitrogen status, was evaluated non-destructively using a SPAD chlorophyll meter (TYS-A, AAULAA, Y230320212, Beijing Jinke Lida Electronic Technology Co., Ltd., Beijing, China), enabling real-time tracking of chlorophyll dynamics across treatments. Measurements were taken from the center of the most recently fully expanded leaf. For each treatment group, three plants were randomly selected, and three readings per plant were averaged. SPAD measurements were conducted at 8:00 AM and 8:00 PM every 7 days throughout the cultivation period to account for diurnal and temporal variation.

Leaf surface temperature was measured using a handheld infrared thermometer (TYS-A, AAULAA), while the photosynthetically active photon flux density (PPFD) at canopy level was recorded using a calibrated quantum sensor (PLA-30, Hangzhou Yuanfang Technology, Hangzhou, China). These environmental parameters were used to verify lighting consistency and assess the microclimate experienced by lettuce plants under the different lighting configurations.

2.5. Statistical Analysis

LED System Performance Metrics

The performance of the LED lighting system was evaluated based on two primary criteria: light uniformity and efficiency.

- Light Uniformity:

The receiving plane, measuring 400 mm × 400 mm, was positioned 500 mm below the light-emitting surface. The PPFD distribution was assessed by dividing the receiving surface into a 5 × 5 grid, comprising 25 evenly distributed measurement points with a spacing of 80 mm between adjacent points. The coefficient of uniformity was calculated using the following equation:

$$\delta\& = \frac{\sum_{x=1}^{X} \sum_{y=1}^{Y} \sum_{n=1}^{N} U/(X \cdot Y \cdot Z)}{K_{\mathrm{PPFDmax}}} \quad (13)$$

To validate the simulation results, actual measurements of photosynthetic photon flux density (PPFD) and color mixing uniformity were conducted using a quantum sensor (PLA-30, Hangzhou Yuanfang) spectrometer in a controlled environment, minimizing external light interference. The LED fixture, measuring 360 × 360 × 1 mm, was positioned 500 mm above the receiving surface to replicate the simulation setup. A grid-based measurement approach was employed, utilizing 25 evenly distributed measurement points arranged in a 5 × 5 grid across the 400 × 400 mm receiving surface, thereby ensuring uniform spatial sampling. Each measurement point was spaced 80 mm apart to accurately capture the PPFD values and assess the PPFD uniformity coefficient.

- Energy Efficiency Assessment

To evaluate the operational sustainability of the lighting system, energy-use efficiency was calculated by comparing total electrical consumption with the corresponding photosynthetically active light output. This metric was used to assess the energy performance of each spectral treatment and to identify configurations with optimal light-use efficiency under controlled cultivation conditions.

- Statistical Analysis

The experiment was structured into seven spectral treatment groups, each consisting of 12 lettuce plants. For each selected plant, all morphological and physiological parameters were measured in triplicate, and the mean values were used for further analysis. The final fresh weight was recorded at harvest, and statistical analysis was conducted using SPSS software (v26.0). One-way analysis of variance (ANOVA) was performed to evaluate differences among treatment means, followed by Tukey's HSD post hoc test to determine statistically significant differences between groups. A threshold of $p < 0.05$ was established to define statistical significance. Since all groups were grown under identical conditions for the same duration, the spectral configuration was the only independent variable tested, justifying the use of one-way ANOVA.

3. Result

3.1. Light Intensity Uniformity Simulation

In Figure 5, Figure 5a presents the simulation results of LED panels arranged according to a particle clustering algorithm in TracePro, while Figure 5c displays the corresponding simulated 3D diagram. Figure 5b illustrates the simulation of traditional LED light sources arranged uniformly in TracePro, where the types and quantities of lamp beads remain consistent. Finally, Figure 5d shows the 3D diagram resulting from this simulation.

Table 2 presents the uniformity performance of two LED array configurations at an irradiation height of 50 cm after optical simulation, evaluated over a 40 cm × 40 cm receiving surface. The PSO-optimized LED array demonstrates superior simulated uniformity (93%), a more consistent photosynthetic photon flux density (PPFD) distribution, and reduced variability in irradiance compared to the traditional uniform LED arrangement, which exhibits greater fluctuations in PPFD values.

Table 2. Uniformity of LED array at 50 cm irradiation height after optical simulation.

LED Arrangement	Number of LEDs	$PPFD_{Avg}$ ($\mu mol \cdot m^{-2} \cdot s^{-1}$)	$PPFD_{Min}$ ($\mu mol \cdot m^{-2} \cdot s^{-1}$)	$PPFD_{Max}$ ($\mu mol \cdot m^{-2} \cdot s^{-1}$)	Illuminance (Lux)	Irradiance (W/m^2)	Simulated Uniformity (%)
PSO-Optimized LED Array	360	200	185	215	550–650	45.6	93
Traditional Uniform LED Array	360	198	160	235	510–650	42.8	83

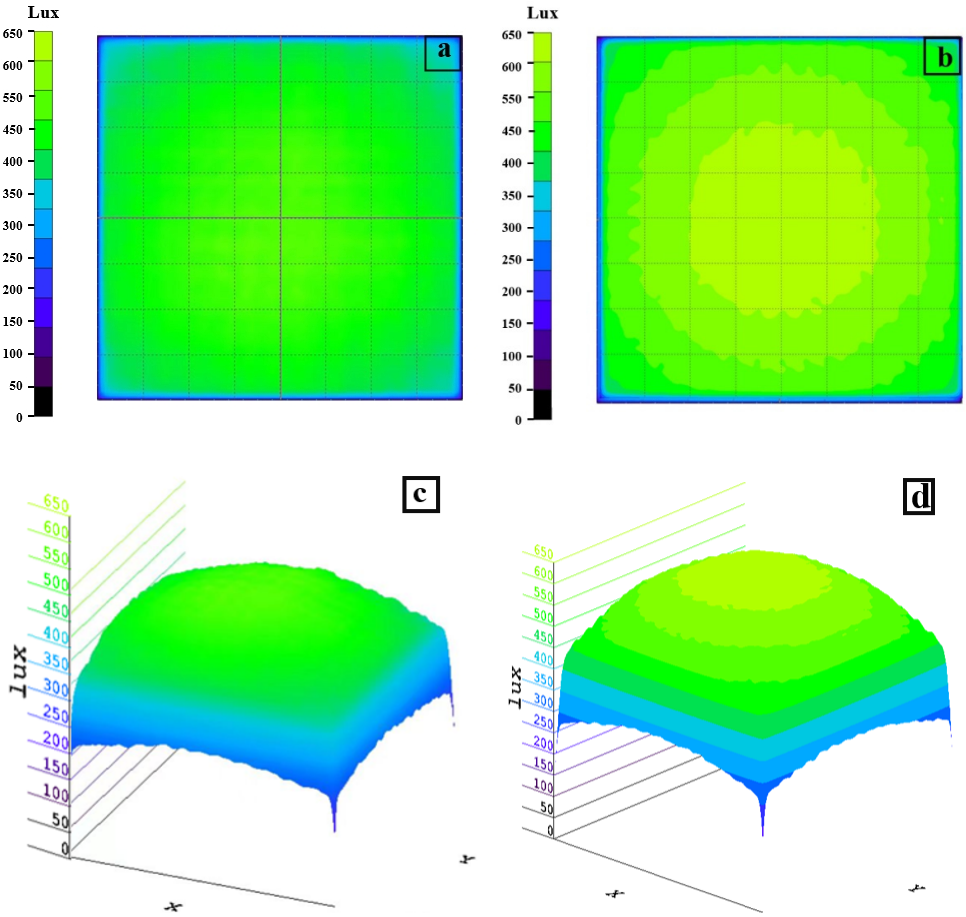


Figure 5. (**a**) Simulated planar irradiance distribution of the LED array layout optimized via the particle swarm optimization (PSO) algorithm, rendered in TracePro; (**b**) simulated planar irradiance distribution of a conventional LED array with uniformly spaced grid placement, utilizing identical LED types and quantities as in (**a**); (**c**) three-dimensional visualization of the irradiance profile corresponding to the PSO-optimized layout, illustrating enhanced spatial uniformity; (**d**) three-dimensional visualization of the irradiance profile for the conventional layout, highlighting non-uniform light distribution patterns.

3.2. Experimental Validation of LED System Performance

The illumination uniformity was quantitatively evaluated on a defined receiving plane, which was evenly divided into 25 rectangular sections of equal area. The center of each section was used as a sampling point for measuring PPFD. These measurements were analyzed using Equations (7) and (8) to assess the system's lighting performance, including spatial uniformity and spectral consistency. The measured uniformity performance of the LED arrays at a 50 cm irradiation height is summarized in Table 3, comparing the PSO-optimized LED array with the traditional uniform LED array across various parameters such as PPFD, illuminance, irradiance, uniformity, PPF, PPE, and PPFUE.

Table 3. Measured uniformity performance of LED arrays at 50 cm irradiation height.

LED Arrangement	Number of LEDs	$PPFD_{Avg}$ ($\mu mol \cdot m^{-2} \cdot s^{-1}$)	$PPFD_{Min}$ ($\mu mol \cdot m^{-2} \cdot s^{-1}$)	$PPFD_{Max}$ ($\mu mol \cdot m^{-2} \cdot s^{-1}$)	Illuminance (lux)	Irradiance (W/m^2)	Uniformity (%)	PPF (mol/s)	PPE (mol/J)	PPFUE (%)
PSO-Optimized LED Array	360	198	180	210	645	44.9	92.5	140	1.9	81
Traditional Uniform LED Array	360	195	155	230	640	42.2	82.7	123	1.6	74

To validate the simulation outcomes, physical measurements were conducted under controlled conditions at an irradiation height of 50 cm, using a 40 cm × 40 cm receiving surface. The performance of the PSO-optimized LED array was compared with that of a traditional uniform LED array in terms of PPFD distribution, irradiance uniformity, and energy utilization. The PSO-optimized system achieved an average PPFD of 198 $\mu mol \cdot m^{-2} \cdot s^{-1}$, slightly higher than the 195 $\mu mol \cdot m^{-2} \cdot s^{-1}$ recorded by the traditional array. Notably, the PSO array exhibited a narrower PPFD range (180–210 $\mu mol \cdot m^{-2} \cdot s^{-1}$) compared to the traditional design (155–230 $\mu mol \cdot m^{-2} \cdot s^{-1}$), indicating improved spatial uniformity. Corresponding illuminance and irradiance values were also enhanced in the PSO system, reaching 645 lux and 44.9 W/m^2, respectively, versus 640 lux and 42.2 W/m^2 in the control group. Furthermore, the PSO-optimized LED array delivered a higher photosynthetic photon flux (PPF) of 120 µmol/s, compared to 109 µmol/s from the traditional setup. The photosynthetic photon flux utilization efficiency (PPFUE) was also significantly improved.

As shown in Figures 6 and 7, the 3D visualizations of PPFD distribution at 40 cm below the LED panels demonstrate a clear difference in light uniformity between the PSO-optimized and traditionally designed systems. The PSO-optimized panel (Figure 6) exhibits a more even light distribution with improved uniformity, while the traditional panel (Figure 7) shows noticeable fluctuations in intensity, indicating less uniform photon delivery across the target area.

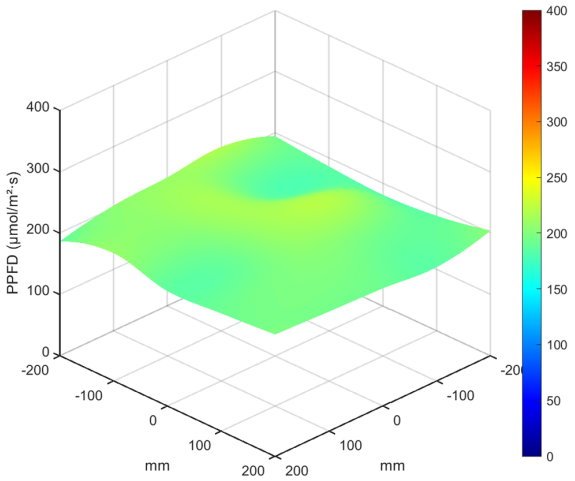


Figure 6. Three-dimensional visualization of PPFD uniformity at 50 cm below the PSO-optimized LED panel, showing improved light distribution and uniformity.

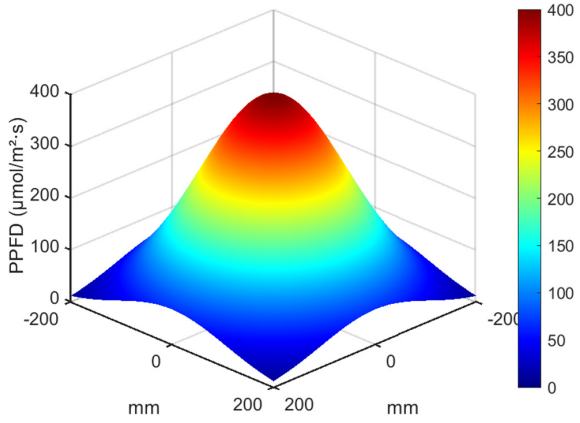


Figure 7. Three-dimensional visualization of PPFD uniformity at 50 cm below the traditionally designed LED panel, illustrating higher variation in light intensity and reduced uniformity.

Figure 8 illustrates the uniformity of photosynthetic photon flux density (PPFD) at varying heights, specifically measured at 20 cm, 30 cm, 40 cm, and 50 cm above the ground in a controlled environment. Table 4 presents the measured photosynthetic photon flux density (PPFD) values, illuminance, irradiance, and signal-to-noise ratio (SNR) at various heights (10 cm, 20 cm, 30 cm, and 40 cm) above the ground. The PPFD values include the average, minimum, and maximum photon flux densities recorded at each height. Additionally, illuminance and irradiance offer further insights into the distribution of light intensity. The SNR values serve to quantify the uniformity of illumination, with higher SNR values indicating greater consistency in light distribution.

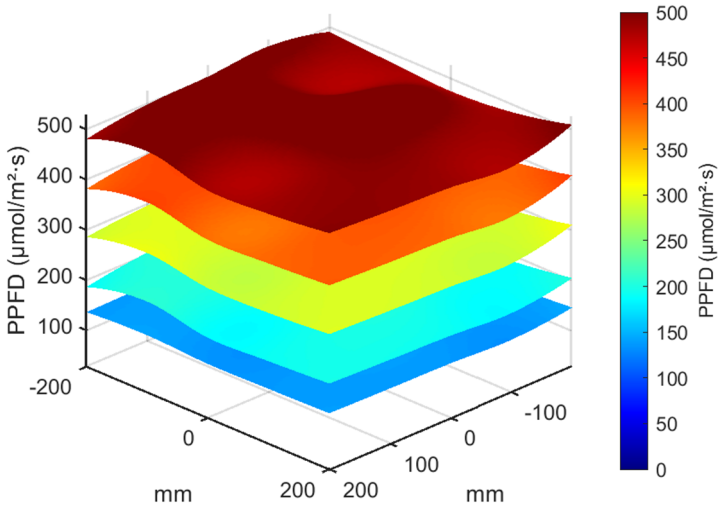


Figure 8. Spatial distribution of PPFD showing high uniformity under the PSO-optimized LED layout.

Table 4. Measured illumination uniformity and SNR at different heights.

Height (cm)	$PPFD_{Avg}$ ($\mu mol \cdot m^{-2} \cdot s^{-1}$)	$PPFD_{Min}$ ($\mu mol \cdot m^{-2} \cdot s^{-1}$)	$PPFD_{Max}$ ($\mu mol \cdot m^{-2} \cdot s^{-1}$)	Uniformity (%)	Irradiance (W/m^2)	SNR (dB)
20 cm	520	470	550	90.3	85.5	49.0
30 cm	430	400	460	93.0	72.1	50.6
40 cm	350	330	380	94.2	60.3	52.8
50 cm	290	275	310	94.8	51.7	54.2

The measured data indicate that PPFD, illuminance, and irradiance decrease as the height above the ground decreases, demonstrating the progressive attenuation and diffusion of light closer to the surface. At a height of 20 cm, the highest PPFD recorded is 550 $\mu mol \cdot m^{-2} \cdot s^{-1}$, accompanied by a signal-to-noise ratio (SNR) of 49.0 dB, suggesting a well-distributed light field with moderate uniformity. As the height decreases to 30 cm, the PPFD reduces to 430 $\mu mol \cdot m^{-2} \cdot s^{-1}$, while the SNR increases to 50.6 dB. At 40 cm, the PPFD further decreases to 350 $\mu mol \cdot m^{-2} \cdot s^{-1}$, and the SNR rises to 52.8 dB, indicating that light uniformity is at its peak at this height, where photon dispersion is optimal. Finally, at 50 cm, the lowest PPFD of 275 $\mu mol \cdot m^{-2} \cdot s^{-1}$ is observed; however, the highest SNR of 54.2 dB confirms that the light field is most uniform at this level, due to reduced scattering and reflection effects near the surface.

3.3. Lettuce Cultivation Test

The analysis of plant height revealed significant differences across the various LED lighting treatments ($p < 0.05$). The measured plant heights under seven different spectral treatments are shown in Figure 9. Error bars represent the standard deviation (SD).

Statistical significance was assessed by one-way ANOVA followed by Tukey's HSD test, where bars sharing the same letter indicate no significant difference, and bars with different letters indicate significant differences ($p < 0.05$). On Day 40, lettuce plants grown under lighting condition E (comprising two violet chips, one blue chip, and 0.21 g of red phosphor) achieved the greatest height, averaging 15.63 cm, which was significantly higher than that of all other treatments. Following closely, Group F (featuring one violet chip, two blue chips, and 0.21 g of red phosphor) exhibited the next highest growth, with an average height of 15.47 cm. In comparison, Group G, which utilized full-spectrum LEDs, presented intermediate values at 15.33 cm. The control group (Group A) recorded the lowest average plant height at 14.60 cm, clearly indicating the growth-promoting effects of integrating violet chips and optimizing phosphor.

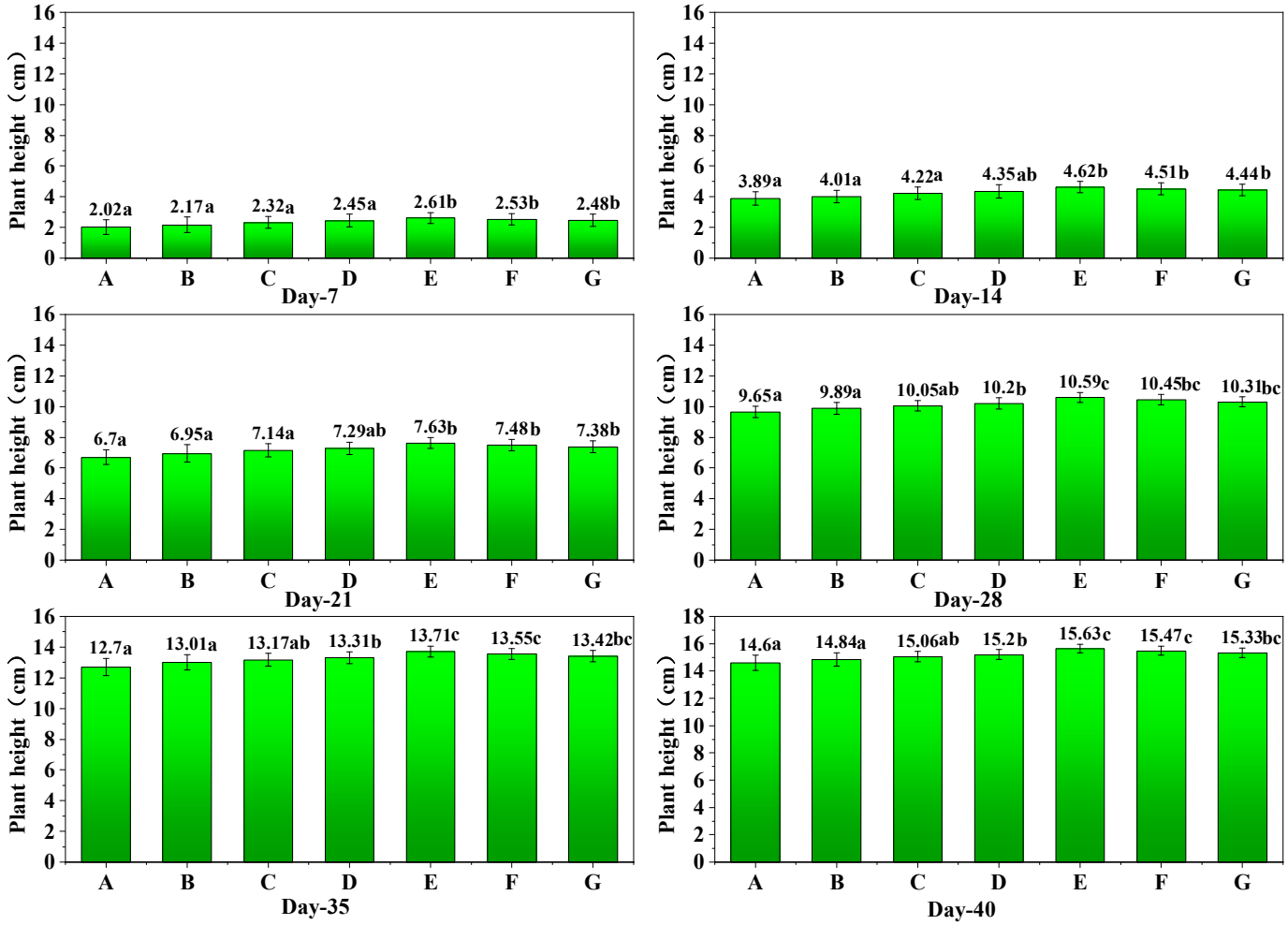


Figure 9. Measured plant height under seven different spectral treatments. Error bars represent the standard deviation (SD). Statistical significance was determined by one-way ANOVA with Tukey's HSD test. Bars with the same letter are not significantly different; bars with different letters differ significantly ($p < 0.05$).

Leaf length exhibited significant variations ($p < 0.05$) across the different treatments. Figure 10 presents the measured leaf lengths across seven experimental groups. Error bars indicate the standard deviation (SD). Statistical significance was evaluated using one-way ANOVA followed by Tukey's HSD test, where bars sharing the same letter are not significantly different, and bars with different letters differ significantly ($p < 0.05$). The longest leaves were observed in Group E on Day 40, measuring an average of 12.35 cm, which was significantly greater than those in the other treatments. Group F followed

closely with an average length of 11.92 cm, while the full-spectrum Group G displayed intermediate leaf lengths of 11.55 cm. The shortest leaves were recorded in Group A, measuring 9.78 cm. These results further validate the beneficial effects of optimized violet-blue light combinations on leaf elongation.

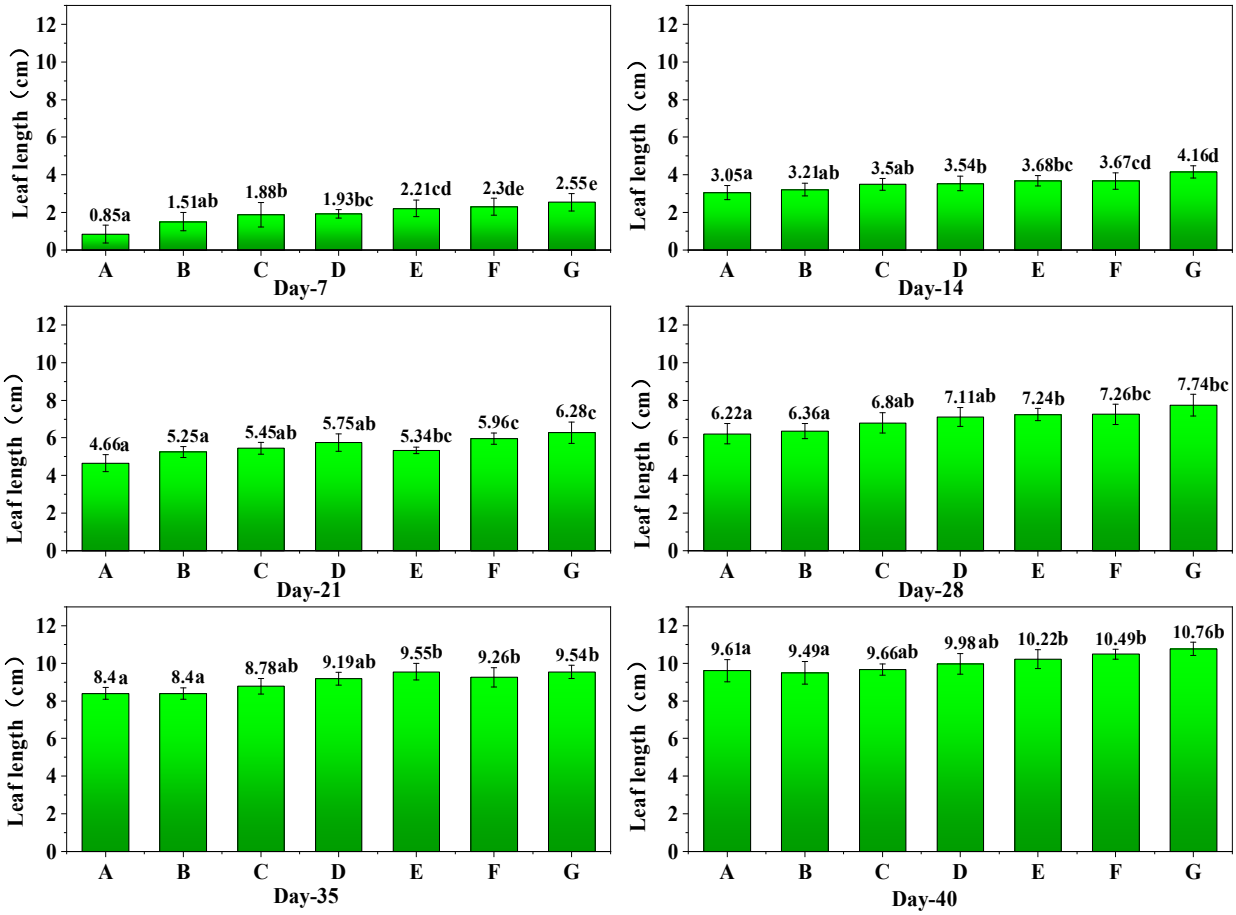


Figure 10. Measured leaf length across seven experimental groups. Error bars represent the standard deviation (SD). Statistical significance was determined by one-way ANOVA with Tukey's HSD test. Bars with the same letter are not significantly different; bars with different letters differ significantly ($p < 0.05$).

Leaf width measurements followed a similar trend as observed for plant height, reinforcing the beneficial effect of the violet–blue LED combination. Figure 11 shows the measured leaf widths across seven experimental groups. Error bars represent the standard deviation (SD). Statistical significance was determined by one-way ANOVA followed by Tukey's HSD test. Bars with the same letter indicate no significant difference, while bars with different letters indicate significant differences ($p < 0.05$). Group E showed the largest average leaf width at Day 40 (10.22 cm), significantly exceeding other groups ($p < 0.05$). Group F and Group G were next, achieving leaf widths of 9.87 cm and 9.52 cm, respectively. Conversely, Group A had the narrowest leaves, with an average width of only 8.02 cm, confirming the limited efficacy of pure blue-light chips combined with minimal red phosphor on lateral leaf expansion.

SPAD values, which indicate leaf relative chlorophyll concentration, revealed significant differences among the lighting treatments ($p < 0.05$). Figure 12 shows the SPAD values measured across four different experimental groups. The box represents the interquartile range (IQR), the line inside the box indicates the median, the whiskers represent the minimum and maximum values, and the small circle inside the box represents the

mean. Notably, Groups E and F exhibited consistently lower SPAD readings throughout the experimental period, averaging approximately 30.0 ± 1.9 and 30.5 at Day 40, respectively. In contrast, the other treatments (Groups A, B, C, D, G) maintained higher SPAD values, averaging around 40.0. The lower SPAD readings observed in the violet-enriched LED treatments (Groups E and F) suggest that these treatments may enhance photosynthetic efficiency, enabling plants to achieve optimal growth with reduced chlorophyll content and potentially lowering the energy costs associated with chlorophyll synthesis.

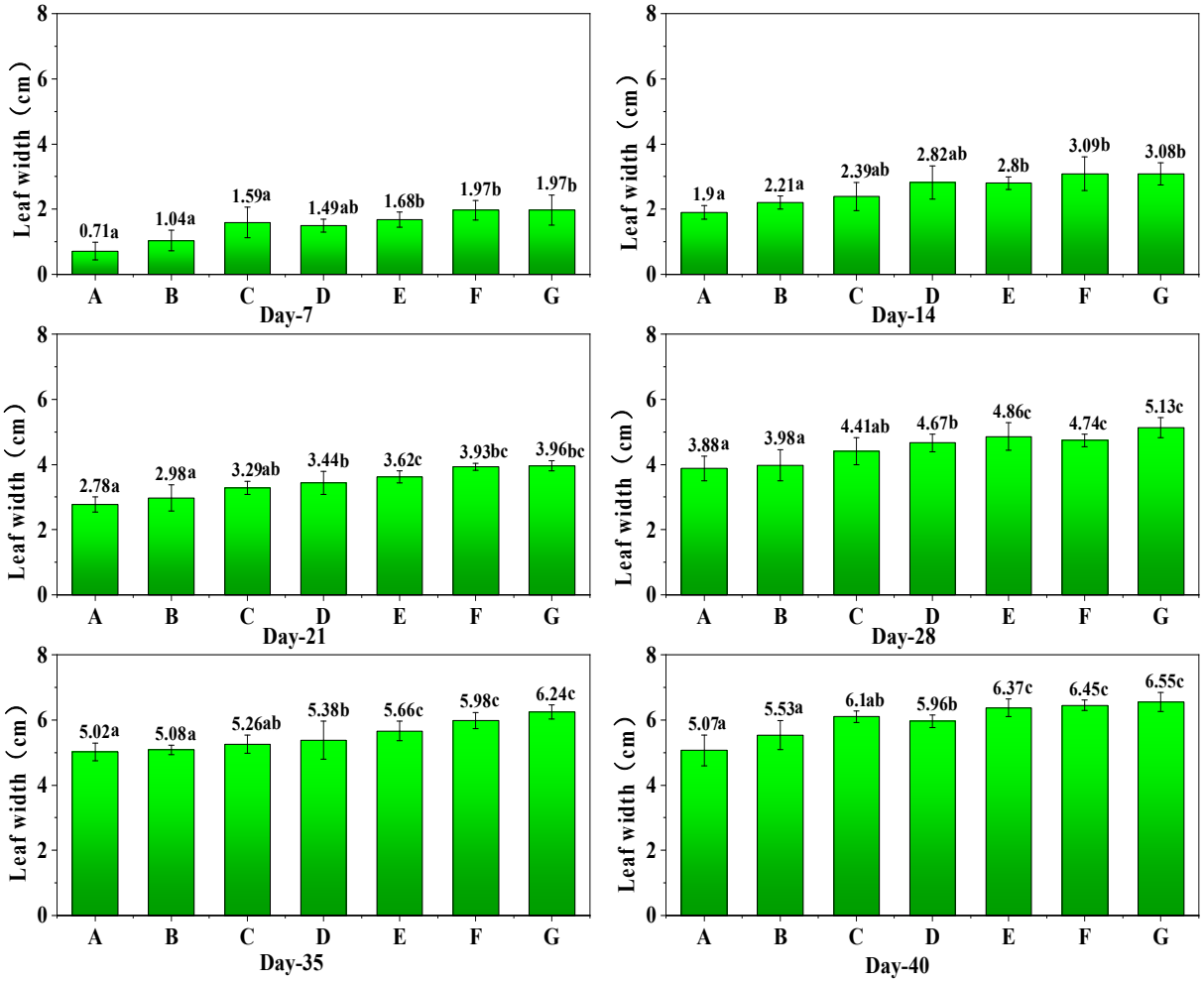


Figure 11. Measured leaf width across seven experimental groups. Error bars represent the standard deviation (SD). Statistical significance was determined by one-way ANOVA with Tukey's HSD test. Bars with the same letter are not significantly different; bars with different letters differ significantly ($p < 0.05$).

Leaf temperature remained stable across all lighting conditions and throughout the experimental duration, averaging 24.0 °C, with no statistically significant differences observed ($p > 0.05$). Table 5 presents a comparison of leaf temperature data measured at multiple time points (Day 7 to Day 40) across six experimental groups (A to F). This result confirmed the effective environmental controls within the miniature plant factory, ensuring that observed growth differences could be attributed exclusively to variations in lighting spectra rather than thermal stress.

Table 5. A comparison of Leaf temperature data.

Leaf Temperature (°C)	Day 7	Day 14	Day 21	Day 28	Day 35	Day 40
A	23.97 ± 0.52	23.57 ± 0.27	24.03 ± 0.38	23.68 ± 0.32	24.20 ± 0.32	23.91 ± 0.48
B	24.18 ± 0.54	24.05 ± 0.42	24.02 ± 0.59	24.08 ± 0.31	24.20 ± 0.40	23.87 ± 0.48
C	23.97 ± 0.64	23.93 ± 0.26	24.01 ± 0.33	24.28 ± 0.46	24.25 ± 0.38	24.09 ± 0.33
D	23.79 ± 0.70	23.98 ± 0.43	24.12 ± 0.57	23.97 ± 0.20	24.09 ± 0.29	24.25 ± 0.28
E	24.09 ± 0.33	23.89 ± 0.39	24.26 ± 0.57	24.37 ± 0.57	24.26 ± 0.32	23.95 ± 0.31
F	23.91 ± 0.29	24.07 ± 0.46	24.10 ± 0.41	23.83 ± 0.25	24.07 ± 0.42	23.94 ± 0.45

Significant variations in fresh weight yield were observed among the treatments ($p < 0.05$). All plants were harvested on Day 40 after transplantation, and fresh weight and energy consumption were recorded on that day. The highest average fresh weight was recorded in Group E, which achieved 90.0 g, representing a substantial yield increase of 25% compared to the control group (Group A, 72.0 g). Groups F and G also exhibited significantly increased fresh weights of 85.0 g (18.1% higher) and 81.0 g (12.5% higher), respectively. In contrast, Group A (72.0 g), which utilized three blue chips combined with the lowest red phosphor concentration, demonstrated the lowest productivity. An analysis of energy consumption further underscored the efficiency of spectral optimization. Group E consumed the least energy (7.3 kWh) among all high-performing groups, notably lower than the energy consumption of Group A (9.2 kWh). Groups F (7.6 kWh) and G (8.2 kWh) also demonstrated lower energy usage compared to conventional lighting setups (A–D).

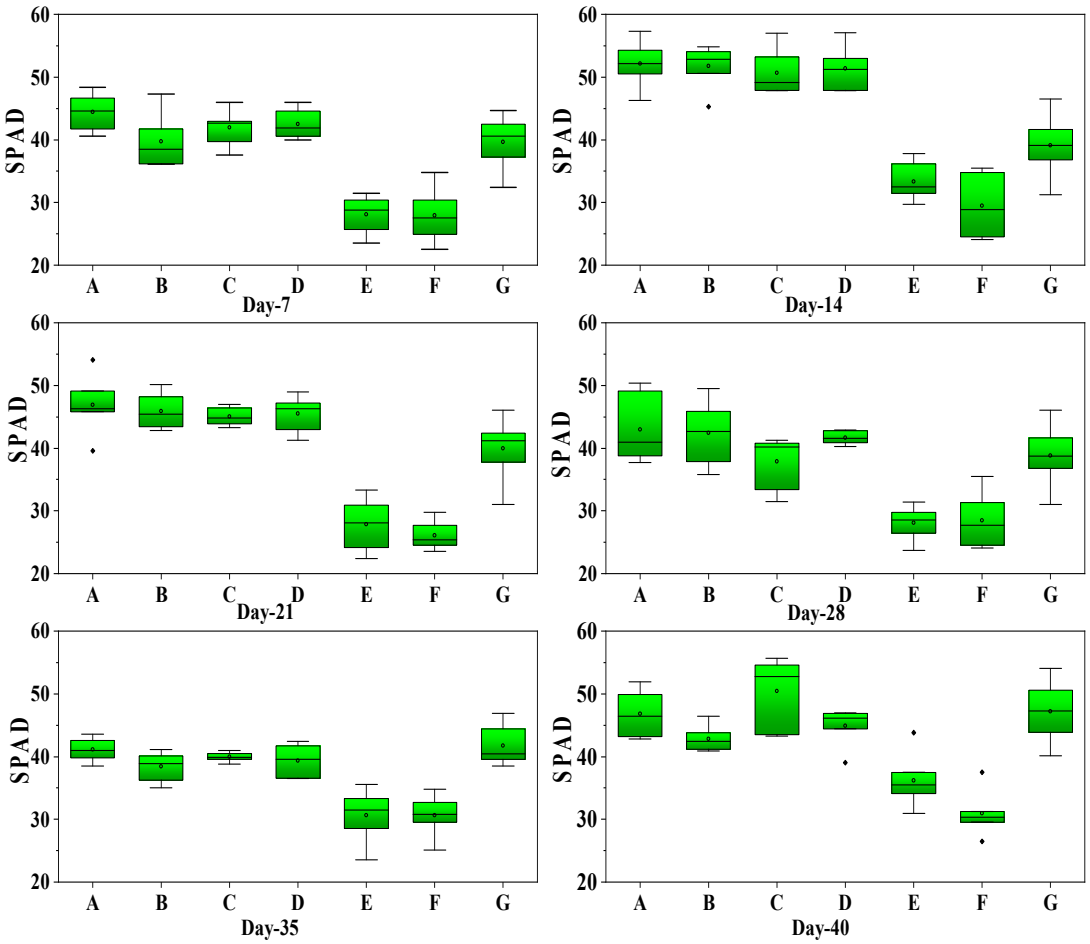


Figure 12. The SPAD measured by four different experimental groups. The box represents the interquartile range (IQR), the line inside the box indicates the median, the whiskers represent the minimum and maximum values, and the small circle inside the box represents the mean value.

4. Discussion

The findings of this study clearly indicate the effectiveness of integrating spectral and spatial optimization through particle swarm optimization (PSO) for enhancing lettuce cultivation in miniature plant factories. Our approach addresses critical challenges highlighted in prior research, particularly related to uniformity of photon distribution, biomass production, and energy efficiency [1,3,4]. For instance, Meng Q et al. investigated the effects of red–blue–white spectra on Romaine lettuce and found that while red–blue combinations increased chlorophyll content and plant height, light uniformity was not considered, which may have led to inconsistent canopy development [21]. In contrast, our study not only tested different spectral compositions, but also applied a PSO-based spatial optimization to improve light distribution, resulting in significantly improved growth uniformity and energy efficiency. Similarly, Mutombo Arcel M examined photosynthetic efficiency under various light spectra and concluded that photon use efficiency decreases with non-uniform PPFD, especially in dense planting systems [22]. Their findings reinforce our observations that uniform PPFD delivery, achieved via layout optimization, can improve photosynthetic consistency across all lettuce samples. Our results also support the work by Zou T, who demonstrated that enhanced vertical light uniformity increases total biomass accumulation in leafy greens grown in vertical stacks [23]. However, unlike their study, which relied on physical reflector configurations, our method achieved comparable or better uniformity through algorithmic control of diode positioning, offering a more scalable and adaptable solution.

In our miniature plant factory setup, the inner walls were intentionally coated with a non-reflective, light-absorbing material to eliminate secondary light reflections and ensure that the measured PPFD and plant growth data reflected only the direct output from the LED arrays. This design choice enabled a more precise evaluation of the spatial and spectral contributions of the lighting system, without interference from wall reflectance. While actual large-scale plant factories often utilize reflective walls to improve light distribution, especially in multi-layer vertical farming systems [24,25], our controlled non-reflective environment was designed to isolate the effects of the spectral–spatial optimization strategy. By minimizing wall-induced photon redistribution, we could more accurately assess the intrinsic lighting uniformity and light-use efficiency of our optimized layout.

Our experimental results demonstrated significant improvements in plant morphological parameters such as height, leaf width, and leaf length, with the highest values recorded under the optimized LED lighting conditions incorporating violet chips and specific phosphor ratios. For example, at Day 40, the plant height under the PSO-optimized violet–blue combination (Group E) reached 15.63 cm, substantially exceeding the 14.60 cm observed under conventional lighting (Group A). This aligns with previous findings by Devesh Singh et al., who observed improved lettuce morphology under optimized red–blue–white LEDs but reported lower uniformity compared to our system [15]. Our spatial optimization achieved a PPFD uniformity of 93%, markedly higher than the 83% reported for traditional LED setups, thus directly addressing a known limitation highlighted by previous studies [26–28]. Furthermore, fresh weight analysis clearly demonstrated significant biomass yield enhancement. Group E achieved an average fresh weight of 90.0 g, reflecting a 25% increase compared to the traditional blue LED treatment (group A, 72.0 g). In contrast, Yung-Sheng Chen reported increases of approximately 15% in biomass yield through physical reflector enhancements in traditional plant factories [17]. Our results thus indicate that spectral–spatial optimization via PSO is substantially more effective, resulting in higher biomass yields coupled with enhanced uniformity. The spectral and spatial distribution of light above the plant canopy differs substantially from that within the canopy due to the optical properties of green leaves. Specifically, green leaves exhibit higher transmittance

and reflectance in the green (500–570 nm) and far-red (700–750 nm) wavebands, while blue (450–495 nm), red (620–700 nm), and UV-A (315–400 nm) photons are absorbed more effectively [29]. This spectral filtering alters both the quality and quantity of light available for photosynthesis and photomorphogenesis in the lower canopy layers [30]. Consequently, the sub-canopy environment is typically enriched in far-red and green light, while being depleted in photosynthetically active blue and red light, which can suppress chlorophyll synthesis and influence leaf morphology [31]. Moreover, reflected far-red light from lower foliage can feedback to the upper canopy, modifying the phytochrome photostationary state and influencing plant architecture through shade-avoidance responses, particularly in dense or heterogeneous canopies [32]. These spatial–spectral interactions contribute to asymmetric light distribution, often resulting in uneven growth even under seemingly uniform external lighting conditions [33]. Although our study utilized a miniature plant factory with fully blacked-out surroundings and non-reflective inner walls to minimize external light interference and inter-reflection, the intrinsic spectral transformations caused by intra-canopy scattering and absorption remain important considerations when interpreting light uniformity and optimizing LED spectra.

Interestingly, SPAD values showed distinct reductions in groups utilizing violet LED chips, averaging around 30.0, compared to approximately 40.0 in blue + red phosphor LED groups. This phenomenon suggests improved photon utilization efficiency under optimized spectra, consistent with the findings from Tomohiro Jishi, who indicated that optimized spectral compositions could reduce unnecessary chlorophyll accumulation and enhance photosynthetic efficiency [24]. Such physiological efficiency likely contributed to the significant biomass increases observed in our optimized treatments. The relationship between SPAD values and light-use efficiency (LUE) is more complex than the conventional assumption that higher SPAD values always indicate higher photosynthetic capacity. Although SPAD measurements are widely used as a proxy for leaf chlorophyll content, recent studies suggest that, under certain environmental conditions, lower SPAD values may be associated with improved LUE [34]. Liu et al. (2023) demonstrated through UAV-based hyperspectral imaging of rice canopies that lower chlorophyll content can lead to more efficient canopy-level light utilization by reducing mutual shading and allowing deeper light penetration within the plant structure [35]. Similarly, Croft et al. (2017) examined multiple species across global ecosystems and found that lower leaf chlorophyll content may correspond with higher proportions of absorbed light being directed toward photosynthesis rather than being lost as thermal dissipation, thereby enhancing LUE [22]. These findings suggest that in some high-light or controlled-environment agriculture scenarios, moderately reduced chlorophyll levels (reflected in lower SPAD values) may actually support higher light-use efficiency by optimizing internal light distribution and minimizing energy loss.

Energy consumption analysis reinforced the benefits of the optimized system, with Group E consuming 7.3 kWh, significantly lower than the conventional system's 9.2 kWh (Group A). This represents a significant improvement in both biomass yield and energy efficiency. The final fresh weight and total energy consumption for each group measured on harvest day (Day 40) are summarized in Table 6. As shown in Table 6, Group E achieved the highest average fresh weight of 90.0 g, corresponding to a 25.0% yield increase compared to the control (Group A: 72.0 g). Importantly, this was accomplished with a 20.7% reduction in energy consumption (7.3 kWh vs. 9.2 kWh). In contrast, other groups such as Group D and Group F also showed notable gains, with 8.3% and 18.1% increases in yield, respectively, while consuming significantly less energy. These results surpass the approximate 10% energy savings previously reported by Huang Yong-ping in LED-optimized plant factories, underscoring the practical value of integrating PSO-based

spectral and spatial LED optimization to simultaneously enhance yield and reduce energy input in controlled-environment agriculture.

Table 6. Final fresh weight and total energy consumption per group (measured on harvest day, Day 40).

Lighting Condition	Fresh Weight$_{avg}$ (g)	Std Dev	Std Error	Energy (kWh)	Yield Increase (%)
Group A	72.0	10.87	1.48	9.2	0.0
Group B	74.0	3.39	0.46	8.8	2.8
Group C	75.0	9.97	1.36	9.5	4.2
Group D	78.0	6.39	0.87	6.1	8.3
Group E	90.0	5.21	0.70	7.3	25.0
Group F	85.0	4.62	0.62	7.6	18.1
Group G	81.0	8.04	1.08	8.2	12.5

Overall, this study provides strong empirical evidence demonstrating the superiority of integrated spectral–spatial optimization through PSO in controlled-environment agriculture, achieving substantial enhancements in photon uniformity, biomass yield, and energy efficiency. This approach effectively addresses previously identified limitations and offers significant potential for scalable implementation in commercial plant factory systems. Nevertheless, several limitations must be acknowledged to better contextualize the broader applicability of these findings. First, the experiment was conducted using a single lettuce cultivar. Although Italian lettuce is widely adopted as a model species in controlled-environment agriculture due to its rapid growth and sensitivity to light quality, plant responses to spectral–spatial light distribution can vary considerably among different cultivars and crop species. Consequently, the generalizability of the results to other genotypes remains uncertain. Future research should validate the proposed optimization strategy across multiple lettuce varieties and diverse high-value crops to ensure robustness and scalability. Second, while morphological characteristics and yield were thoroughly quantified, the study did not evaluate fresh product quality. Critical quality parameters—including nutrient composition (e.g., vitamin C content, nitrate levels), water and fiber content, and head structure—were not assessed. These factors are essential for commercial adoption, as they influence marketability, shelf life, and consumer satisfaction. Without these assessments, the implications of yield enhancement remain only partially understood. Future work should integrate both quantitative and qualitative metrics to provide a more comprehensive evaluation of lighting strategies in plant factory systems.

5. Conclusions

This study presents a comprehensive approach to optimizing artificial lighting conditions for lettuce cultivation in miniature plant factories by combining spectral tailoring with spatial distribution optimization using particle swarm optimization (PSO). By accurately determining the spectral absorption characteristics of Italian lettuce, we identified key photosynthetically active wavelength bands, notably in the blue (450–470 nm) and red (640–670 nm) regions. Based on this, analysis, we developed seven custom LED spectral treatments were developed, including combinations of blue and violet chips with precise concentrations of red phosphor, alongside a full-spectrum control.

Spectral customization significantly influenced plant morphology and physiology. The treatment combining two violet chips, one blue chip, and 0.21 g of red phosphor (Group E) yielded the most favorable outcomes, achieving a maximum fresh weight of 90.0 g per plant, representing a 25% increase over the traditional blue-light control (Group A, 72.0 g). This enhancement was accompanied by increased plant height (15.63 cm), wider leaves (10.22 cm), and longer leaf blades (12.35 cm), indicating comprehensive vegetative growth

promotion. Meanwhile, SPAD values in Groups E and F were significantly lower (~30) than in conventional lighting treatments (~40), suggesting improved light-use efficiency with reduced chlorophyll oversaturation. To ensure that optimized spectral conditions were uniformly delivered across the cultivation plane, a PSO algorithm was implemented to optimize the spatial layout of LED arrays. Simulation and experimental validation demonstrated that the optimized design achieved a PPFD uniformity of 93%, notably higher than the 83% of conventional designs. This uniformity directly contributed to consistent growth across all lettuce samples. Energy analysis further highlighted the system's efficiency: Group E consumed only 7.3 kWh while producing the highest yield, compared to 9.2 kWh in the control group. This demonstrates the feasibility of improving biomass production while simultaneously reducing energy input through integrated optimization strategies.

In summary, this research demonstrates that a synergistic approach—grounded in plant absorption spectrum analysis, spectral customization, and algorithmic spatial design—can substantially enhance light utilization, crop uniformity, and energy efficiency in indoor horticulture systems. These findings lay a solid foundation for the development of scalable, high-performance, and sustainable LED lighting solutions for vertical farming and controlled-environment agriculture.

Author Contributions: Conceptualization: J.Z.; Methodology: J.Z. and M.S.; Software: Z.W.; Validation: H.H., J.W. and Z.W.; Formal analysis: H.H. and Y.X.; Investigation: Z.W.; Resources: J.Z.; Data curation: Z.W.; Writing—original draft: Z.W.; Writing—review and editing: J.Z. and M.S.; Visualization: Z.W.; Supervision: J.Z. and M.S.; Project administration: J.Z.; Funding acquisition: J.Z.; Literature search: M.S. and Y.W. All authors have read and agreed to the published version of the manuscript.

Funding: This research was financially supported by Shanghai Science and Technology Committee (STCSM) Science and Technology Innovation Program (Grant No. 23N21900100). Shanghai Science and Technology Committee (STCSM) Science and Technology Innovation Program (Grant No. 22N21900400).

Data Availability Statement: Data underlying the results presented in this paper are not publicly available at this time but may be obtained from the authors upon reasonable request.

Conflicts of Interest: The authors declare no conflicts of interest.

References

1. He, D.; Wu, Q.; Feng, C.; Xu, J.; Van Labeke, M.C. Light quality and plant development in controlled environments: A review on lettuce as a model. *Front. Plant Sci.* **2020**, *11*, 592171. [CrossRef]
2. Abedi, M.; Tan, X.; Stallknecht, E.J.; Runkle, E.S.; Klausner, J.F.; Murillo, M.S.; Bénard, A. Incorporating the effect of the photon spectrum on biomass accumulation of lettuce using a dynamic growth model. *Front. Plant Sci.* **2023**, *14*, 1106576. [CrossRef] [PubMed]
3. Lim, E.; Kim, J.O.; Oh, M.M. Optimizing the photon ratio of red, green, and blue LEDs for lettuce seedlings: A mixture design approach. *Plant Methods* **2023**, *19*, 121. [CrossRef] [PubMed]
4. Alrajhi, A.A.; Alsahli, A.S.; Alhelal, I.M.; Rihan, H.Z.; Fuller, M.P.; Alsadon, A.A.; Ibrahim, A.A. The Effect of LED Light Spectra on the Growth, Yield and Nutritional Value of Red and Green Lettuce (*Lactuca sativa*). *Plants* **2023**, *12*, 463. [CrossRef] [PubMed]
5. Lozano-Castellanos, L.F.; Navas-Gracia, L.M.; Correa-Guimaraes, A. Light Energy Efficiency in Lettuce Crop: Structural Indoor Designs Simulation. *Plants* **2023**, *12*, 3456. [CrossRef]
6. Sawatdee, S.; Jarunglumlert, T.; Pavasant, P.; Sakihama, Y.; Flood, A.E.; Prommuak, C. Effect of mixed light emitting diode spectrum on antioxidants content and antioxidant activity of red lettuce grown in a closed soilless system. *BMC Plant Biol.* **2023**, *23*, 351. [CrossRef]
7. Briglia, N.; Zhen, S.; van Iersel, M.W. Optimizing Light Use Efficiency to Improve Yield and Energy Efficiency in Controlled Environment Agriculture. *Agronomy* **2024**, *14*, 224. [CrossRef]
8. Baeza, E.; Litago, J.; Alonso, J.L. Assessing the Energy Efficiency of LED Lighting Systems in Indoor Agriculture: A Light Use Efficiency Approach. *Food Energy Secur.* **2022**, *11*, e391. [CrossRef]

9. Chen, R.; Wang, Z.; Liu, W.; Ding, Y.; Zhang, Q.; Wang, S. Side Lighting of Red, Blue and Green Spectral Combinations Altered the Growth, Yield and Quality of Lettuce (*Lactuca sativa* L. cv. "Yidali") in Plant Factory. *Plants* **2023**, *12*, 4147. [CrossRef]
10. Zou, T.; Huang, C.; Wu, P.; Ge, L.; Xu, Y. Optimization of Artificial Light for Spinach Growth in Plant Factory Based on Orthogonal Test. *Plants* **2020**, *9*, 490. [CrossRef]
11. Lee, J.H.; Kwon, Y.B.; Roh, Y.H.; Choi, I.-L.; Kim, J.; Kim, Y.; Yoon, H.S.; Kang, H.-M. Effect of Various LED Light Qualities, Including Wide Red Spectrum-LED, on the Growth and Quality of Mini Red Romaine Lettuce (cv. Breen). *Plants* **2023**, *12*, 2056. [CrossRef]
12. Huang, W.-T.; Su, T.-Y.; Chuang, J.-H.; Lu, K.-M.; Hu, S.-F.; Liu, R.-S. Plant Growth Modeling and Response from Broadband Phosphor-Converted Lighting for Indoor Agriculture. *ACS Appl. Mater. Interfaces* **2023**, *15*, 32589–32596. [CrossRef]
13. Gómez, C.; Mitchell, C.A. Growth Responses of Tomato Seedlings to Different Spectra of Supplemental Lighting. *Hortscience* **2015**, *50*, 112–118. [CrossRef]
14. Arcel, M.M.; Lin, X.; Huang, J.; Wu, J.; Zheng, S. The application of LED illumination and intelligent control in plant factory, a new direction for modern agriculture: A Review. *J. Phys. Conf. Ser.* **2021**, *1732*, 012178. [CrossRef]
15. Singh, D.; Basu, C.; Meinhardt-Wollweber, M.; Roth, B. LEDs for energy efficient greenhouse lighting. *Renew. Sustain. Energy Rev.* **2015**, *49*, 139–147. [CrossRef]
16. Zheng, J.; Ji, F.; He, D.; Niu, G. Effect of Light Intensity on Rooting and Growth of Hydroponic Strawberry Runner Plants in a LED Plant Factory. *Agronomy.* **2019**, *9*, 875. [CrossRef]
17. Chen, Y.-S.; Lin, C.-Y.; Yeh, C.-M.; Kuo, C.-T.; Hsu, C.-W.; Wang, H.-C. Anti-glare LED lamps with adjustable illumination light field. *Opt. Express* **2014**, *22*, 5183. [CrossRef] [PubMed]
18. Huang, Y.-S.; Luo, W.-C.; Wang, H.-C.; Feng, S.-W.; Kuo, C.-T.; Lu, C.-M. How Smart LEDs Lighting Benefit Color Temperature and Luminosity Transformation. *Energies* **2017**, *10*, 518. [CrossRef]
19. Li, H.; Sang, X. LED array light source illuminance distribution and photoelectric detection performance analysis in dust concentration testing system. *Sens. Actuators A Phys.* **2018**, *271*, 111–117. [CrossRef]
20. Huang, Y.; Ma, J. Laser and LED Hybrid Plant Lighting System Design Based on the Particle Swarm Algorithm. *Appl. Sci.* **2020**, *10*, 7588. [CrossRef]
21. Meng, Q.; Runkle, E.S. Blue Photons from Broad-Spectrum LEDs Control Growth, Morphology, and Coloration of Indoor Hydroponic Red-Leaf Lettuce. *Plants* **2023**, *12*, 1127. [CrossRef] [PubMed]
22. Croft, H.; Chen, J.M.; Luo, X.; Bartlett, P.; Chen, B.; Staebler, R.M. Leaf chlorophyll content as a proxy for leaf photosynthetic capacity. *Glob. Change Biol.* **2017**, *23*, 3513–3524. [CrossRef] [PubMed]
23. Soufi, H.R.; Roosta, H.R.; Stępień, P.; Malekzadeh, K.; Hamidpour, M. Manipulation of light spectrum is an effective tool to regulate biochemical traits and gene expression in lettuce under different replacement methods of nutrient solution. *Sci. Rep.* **2023**, *13*, 8600. [CrossRef] [PubMed]
24. Zou, H.; Li, C.; Zhang, A.; Zhang, X.; Chen, X.; Wang, F.; Yan, Y.; Zhang, S. Light environment control for reducing energy loss and increasing crop yield in plant factories. *Sol. Energy* **2024**, *268*, 112281. [CrossRef]
25. Agati, G.; Franchetti, B.; Rispoli, F.; Venturini, P. Thermo-fluid dynamic analysis of the air flow inside an indoor vertical farming system. *Appl. Therm. Eng.* **2024**, *236*, 121553. [CrossRef]
26. Zhou, Y.; Xu, Y.; Ji, Z.; Zhou, G. Optimal Design of Red, Blue, and Far-Red LEDs Array. *Prog. Electromagn. Res. C* **2018**, *81*, 181–189. [CrossRef]
27. Williams, L.E. A light salad [LED lighting applications in horticulture]. *Eng. Technol.* **2018**, *13*, 50–53. [CrossRef]
28. Su, Z.; Xue, D.; Ji, Z. Designing LED array for uniform illumination distribution by simulated annealing algorithm. *Opt. Express* **2012**, *20*, A843. [CrossRef]
29. Jishi, T.; Fujiwara, K. Time-varying Photosynthetic Photon Flux Density and Relative Spectral Photon Flux Density Distribution to Improve Plant Growth and Morphology in Plant Factories with Artificial Lighting. *Hortic. J.* **2021**, *90*, 147–153. [CrossRef]
30. Wang, Q.-W.; Robson, T.M.; Pieristè, M.; Kenta, T.; Zhou, W.; Kurokawa, H. Canopy structure and phenology modulate the impacts of solar radiation on C and N dynamics during litter decomposition in a temperate forest. *Sci. Total Environ.* **2022**, *820*, 153185. [CrossRef]
31. González, C.V.; Jeréz, D.N.; Jofré, M.F.; Guevara, A.; Prieto, J.; Mazza, C.; Williams, L.E.; Giordano, C.V. Blue light attenuation mediates morphological and architectural acclimation of Vitis vinifera cv. Malbec to shade and increases light capture. *Environ. Exp. Bot.* **2019**, *157*, 112–120. [CrossRef]
32. Zhang, N.; van Westreenen, A.; He, L.; Evers, J.B.; Anten, N.P.R.; Marcelis, L.F.M. Light from below matters: Quantifying the consequences of responses to far-red light reflected upwards for plant performance in heterogeneous canopies. *Plant Cell Environ.* **2020**, *44*, 102–113. [CrossRef] [PubMed]
33. Huber, M.; Nieuwendijk, N.M.; Pantazopoulou, C.K.; Pierik, R. Light signalling shapes plant–plant interactions in dense canopies. *Plant Cell Environ.* **2020**, *44*, 1014–1029. [CrossRef] [PubMed]

34. Arcel, M.M.; Yousef, A.F.; Shen, Z.H.; Nyimbo, W.J.; Zheng, S.H. Optimizing lettuce yields and quality by incorporating movable downward lighting with a supplemental adjustable sideward lighting system in a plant factory. *PeerJ* **2023**, *11*, e15401. [CrossRef]
35. Liu, H.; Lei, X.; Liang, H.; Wang, X. Multi-Model Rice Canopy Chlorophyll Content Inversion Based on UAV Hyperspectral Images. *Sustainability* **2023**, *15*, 7038. [CrossRef]

Disclaimer/Publisher's Note: The statements, opinions and data contained in all publications are solely those of the individual author(s) and contributor(s) and not of MDPI and/or the editor(s). MDPI and/or the editor(s) disclaim responsibility for any injury to people or property resulting from any ideas, methods, instructions or products referred to in the content.